


Intrinsic Z-DNA Is Stabilized by the Conformational Selection Mechanism of Z-DNA-Binding Proteins

Sangsu Bae,^{†,‡} Doyoun Kim,[§] Kyeong Kyu Kim,^{*,§} Yang-Gyun Kim,^{*,||} and Sungchul Hohng^{*,†,‡,⊥}

[†]Department of Physics and Astronomy, [‡]National Center for Creative Research Initiatives, and [⊥]Department of Biophysics and Chemical Biology, Seoul National University, Seoul 151-747, Korea

[§]Department of Molecular Cell Biology, Samsung Biomedical Research Institute, Sungkyunkwan University School of Medicine, Suwon, Gyeonggi 440-746, Korea

^{||}Department of Chemistry, Sungkyunkwan University, Suwon, Gyeonggi 440-746, Korea

 Supporting Information

ABSTRACT: Z-DNA, a left-handed isoform of Watson and Crick's B-DNA, is rarely formed without the help of high salt concentrations or negative supercoiling. However, Z-DNA-binding proteins can efficiently convert specific sequences of the B conformation into the Z conformation in relaxed DNA under physiological salt conditions. As in the case of many other specific interactions coupled with structural rearrangements in biology, it has been an intriguing question whether the proteins actively induce Z-DNAs or passively trap transiently preformed Z-DNAs. In this study, we used single-molecule fluorescence assays to observe intrinsic B-to-Z transitions, protein association/dissociation events, and accompanying B-to-Z transitions. The results reveal that intrinsic Z-DNAs are dynamically formed and effectively stabilized by Z-DNA-binding proteins through efficient trapping of the Z conformation rather than being actively induced by them. Our study provides, for the first time, detailed pictures of the intrinsic B-to-Z transition dynamics and protein-induced B-to-Z conversion mechanism at the single-molecule level.

Specificity is a premise of life, and highly specific interactions are ubiquitous in many biological interactions, including protein–DNA, protein–protein, protein–metabolite, and other interactions. The lock-and-key model was proposed to explain the high specificity of molecular recognition by a precise structural fit of interacting molecules.¹ In most specific interactions, however, the formation of molecular complexes is coupled with small- or large-scale structural rearrangements.^{2–4} Two representative mechanisms have been envisioned for the achievement of the final precise fit: in the “induced fit” model, initial binding actively starts the development of the structural change,⁵ and in the “conformational selection” model, a pre-existing precise fit becomes a dominant structure through a passive but selective stabilization process.⁶ Even though it is a fundamental question which pathway is actually used to achieve a final match in many specific molecular interactions, experimental evidence is rare and controversies are still ongoing.^{7–12}

The structural transition between right-handed B-DNA¹³ and left-handed Z-DNA^{14,15} (i.e., the B-to-Z transition) is such an

example. Left-handed Z-DNA is preferably formed in purine–pyrimidine repeats at extremely high salt concentrations *in vitro*¹⁶ or with the help of negative supercoiling *in vivo*.¹⁷ Alternatively, recent studies have revealed that the B-to-Z transition can also be mediated by Z-DNA-binding proteins (ZBPs),^{18–21} providing a good model system to answer the compelling question of whether the proteins actively induce Z-DNAs or passively trap preformed Z-DNAs.²² One conceivable way to most directly answer the question is to study the ZBP's effect on the intrinsic B-to-Z transition dynamics, if there is any. Recently, fluorescence resonance energy transfer (FRET) assays^{23,24} were developed to detect salt- or supercoiling-induced B-to-Z transitions at the single-molecule level.²⁵ In this work, we applied the single-molecule FRET technique to observe the real-time dynamics of intrinsic B-to-Z transitions under low-salt and relaxed conditions, ZBP binding/dissociation events, and the accompanying B-to-Z transitions.

For single-molecule FRET experiments, we prepared dye-labeled DNA duplexes comprising a CG repeat (gray and yellow in Figure 1a) and a flanking random sequence (blue in Figure 1a) by annealing the following DNA strands: 5'-/Cy3/CGCGC-GCGCGCGATAACCCACC/biotin/-3' and 5'-GGTGGGTT-AT^{Cy3}CGCGCGCGCGCG-3'. The thymine base at the B–Z junction (red in Figure 1a), which is flipped out in the Z form,²⁶ was selected as the labeling position of the donor (Cy3) to maximize the FRET change during the B-to-Z transition. Annealed DNA molecules were immobilized on a polymer-coated quartz surface by the biotin–streptavidin interaction, and the fluorescence signals of the donor and acceptor were obtained using a wide-field total-internal-reflection fluorescence microscope (Figure 1a).²⁴

First, we studied the B-to-Z transition initiated by the binding of the Z α domain of human double-stranded RNA adenosine deaminase (hZ α _{ADAR1}), which is one of the most efficient Z-DNA-inducing proteins and for which a wealth of biochemical and structural information is available. Figure 1b shows FRET histograms of the DNA duplexes after incubation for 30 min with various concentrations of hZ α _{ADAR1}. In the absence of hZ α _{ADAR1}, the FRET histogram was well-fitted by a single Gaussian distribution, confirming the existence of a single conformation (i.e., B-DNA). For hZ α _{ADAR1} concentrations

Received: August 19, 2010

Published: December 20, 2010

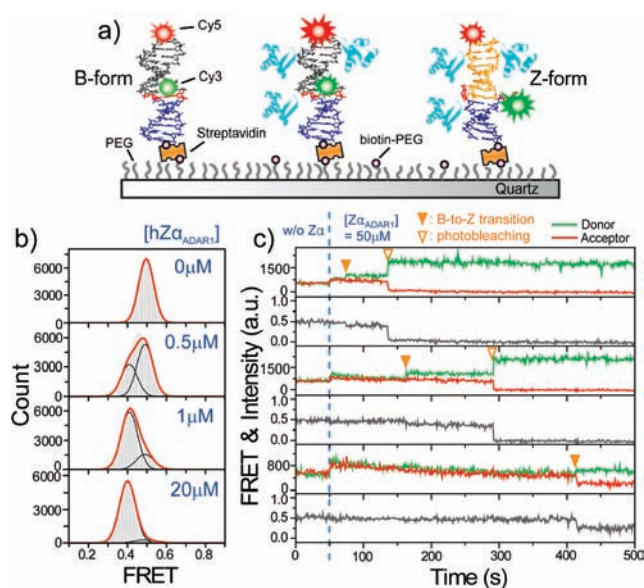


Figure 1. Stepwise but delayed protein-induced B-to-Z transition. (a) Experimental scheme. DNA duplexes comprising a random-sequence region (blue) and a flanking CG repeat were immobilized on a polymer-coated quartz surface by the biotin–streptavidin interaction. As the CG repeat switches between the B form (gray) and the Z form (yellow), simultaneous FRET fluctuations are expected. (b) FRET histograms at various $hZ\alpha_{ADAR1}$ concentrations ($T = 25^\circ\text{C}$). (c) Buffer exchange experiments. At 50 s (blue dashed line), $50\ \mu\text{M}$ $hZ\alpha_{ADAR1}$ was rapidly delivered into a detection chamber. The instantaneous intensity increase of the donor (green lines) and acceptor (red lines) indicates that the binding equilibrium of $Z\alpha$ proteins is rapidly established ($<1\ \text{s}$). FRET transitions (orange ∇ in Figure 1c) occur with time delays in a stepwise manner. Yellow ∇ indicate photobleaching of acceptors.

above $0.5\ \mu\text{M}$, however, a low-FRET peak started to appear and then became a dominant state at higher protein concentrations. Circular dichroism measurements confirmed that the B-to-Z transition actually occurred in this sample with the addition of $hZ\alpha_{ADAR1}$ (Figure S1 in the Supporting Information). In contrast, experiments with a random DNA duplex (Figure S2) and a DNA duplex with 12 consecutive C–G pairs (Figure S3) as negative controls did not show such a low-FRET state, identifying the low-FRET peak in Figure 1b as Z-DNA.

After the successful establishment of a single-molecule monitoring system for the protein-induced B-to-Z transitions, we investigated details of the B-to-Z transition in the presence of $hZ\alpha_{ADAR1}$. While observing single-molecule fluorescence images of DNA duplexes, we rapidly delivered $hZ\alpha_{ADAR1}$ at the saturation concentration ($50\ \mu\text{M}$) into the detection chamber (blue dashed line in Figure 1c). The instantaneous fluorescence-intensity jumps indicated rapid binding of $hZ\alpha_{ADAR1}$ to DNA duplexes.²⁷ However, FRET changes corresponding to B-to-Z transitions (orange ∇ in Figure 1c) occurred in a stepwise manner with long time delays (5.4 min average transition time; Figure S4).

To determine whether $hZ\alpha_{ADAR1}$ plays an active or passive role in this B-to-Z transition, it is important to compare the intrinsic B-to-Z transition rate with the transition rate in the presence of $hZ\alpha_{ADAR1}$. Since $hZ\alpha_{ADAR1}$ did not work under high salt conditions (data not shown), we needed to find low-salt conditions under which intrinsic Z-DNA is formed. To increase the probability of Z-DNA formation under low-salt conditions,

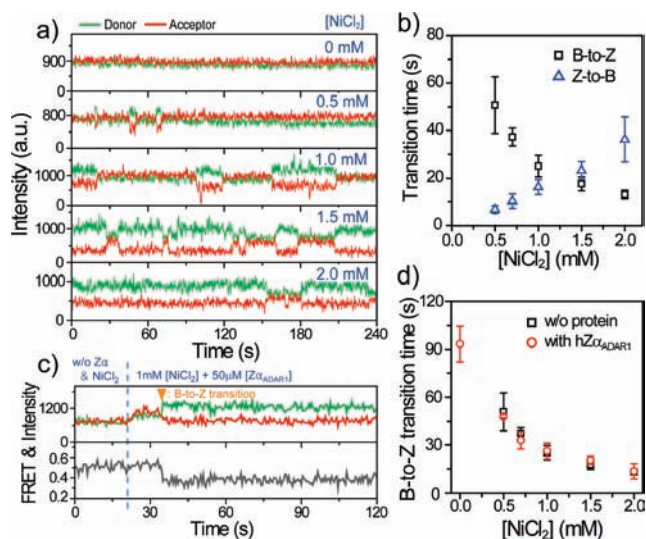


Figure 2. Passive trapping rather than active inducing. (a) Intrinsic B-to-Z transition dynamics of cytosine-methylated DNA duplexes. Typical fluorescence intensity time traces of the donor (green lines) and acceptor (red lines) at various Ni^{2+} concentrations are shown. (b) Dwell times of the B form (black \square) and Z-form (blue \triangle) at various Ni^{2+} concentrations. (c) Representative fluorescence intensity time traces of the donor (green lines) and acceptor (red lines) in $hZ\alpha_{ADAR1}$ delivery experiments. (d) Comparison of B-to-Z transition times in the presence (red \circ) and absence (black \square) of $hZ\alpha_{ADAR1}$ at various Ni^{2+} concentrations. All of the experiments were performed at 37°C .

we prepared another DNA duplex containing 5-methyl dCs in the CG repeat²⁸ and tested various multivalent ions for the ability to induce Z-DNA at low salt concentrations. When millimolar Ni^{2+} ions were added, DNA duplexes started to repeatedly switch between the B form (the high-FRET state) and the Z form (the low-FRET state) (Figure 2a), whereas such a FRET transition was not observed with other multivalent ions (Figure S5).²⁹ This is the first time that B–Z transitions have been observed for relaxed DNA, allowing us to determine the intrinsic B–Z transition rates by analyzing the dwell times in the B and Z forms (Figures S6 and S7). With escalating Ni^{2+} concentration, the Z-DNA dwell time increased linearly whereas the B-DNA dwell time monotonically decreased (Figure 2b).

After determining the intrinsic B–Z transition rates at various Ni^{2+} concentrations, we investigated the effect of $hZ\alpha_{ADAR1}$ binding on the B-to-Z transition rates by rapidly delivering both $hZ\alpha_{ADAR1}$ ($50\ \mu\text{M}$) and Ni^{2+} into the detection chamber. As in the case of the unmethylated DNA substrate, the fluorescence intensities instantaneously increased after the protein injection, indicating rapid binding of $hZ\alpha_{ADAR1}$, while actual B-to-Z transitions occurred with time delays after the protein binding (Figure 2c and Figure S8). Comparison of these time delays with the intrinsic B-to-Z transition times showed a remarkable similarity over the whole range of Ni^{2+} concentrations tested (Figure 2d), clearly demonstrating that $hZ\alpha_{ADAR1}$ does not accelerate Z-DNA formation. We obtained the same result with another ZBP³⁰ (Figure S9) and a different Z-DNA-forming sequence (Figure S10). Thus, this conclusion seems to be general, although further systematic studies with different DNA sequences and other ZBPs would be needed to make the result more conclusive. In the absence of Ni^{2+} ions, we could not directly observe intrinsic B-to-Z transitions, but the protein-assisted B-to-Z transition was still efficient. The combination of

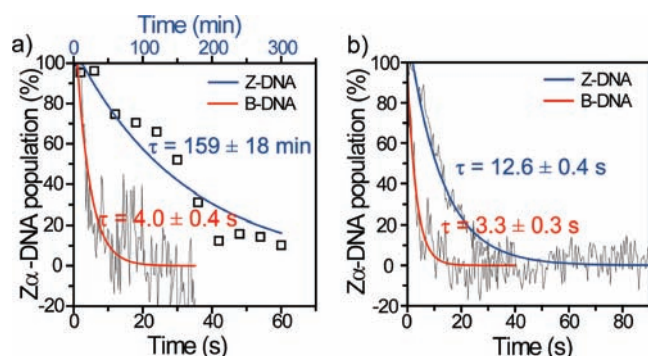


Figure 3. Origin of specificity. (a) Curves for dissociation of hZα_{ADAR1} from Z-DNA (black □) and B-DNA (black line) were obtained from rapid buffer exchange experiments in Figures S11 and S12. The dissociation times were obtained by fitting the data to single-exponential curves (blue for Z-DNA and red for B-DNA). (b) Curves for dissociation of hZα_{Y177F} from Z-DNA and B-DNA (black lines) were obtained from rapid buffer exchange experiments in Figure S13. The dissociation times were obtained by fitting the data to single-exponential curves (blue for Z-DNA and red for B-DNA). All of the experiments were performed at 25 °C.

two observations, namely, the conformational selection mechanism of ZBPs in the B-to-Z transition and the efficient conversion of relaxed B-DNA into Z-DNA under low-salt conditions by ZBPs, strongly suggests that intrinsic B-to-Z transition dynamics really exists in the relaxed state of DNA at physiological salt concentrations and that ZBPs thereby efficiently trap even undetectably low amounts of transient Z-DNAs.

The fact that ZBPs play a passive role in the B-to-Z transition suggests that ZBPs may have a strong binding affinity to preformed Z-DNAs. To study the conformational specificity of ZBPs in the dissociation step, we compared dissociation times of ZBPs from B-DNA and Z-DNA. To measure the dissociation time of hZα_{ADAR1} from Z-DNA, we initially converted all of the DNAs into the Z form by incubating the unmethylated DNA duplexes for 1 h with 50 μM hZα_{ADAR1} and then removed free hZα_{ADAR1} from the detection channel. The protein dissociation times were calculated from the time-lapse FRET histograms (Figure S11). To measure the protein dissociation times for B-form DNA, we incubated the DNA duplexes with 50 μM hZα_{ADAR1} for 5 min, a time long enough to establish a binding equilibrium but short enough for an appreciable amount of DNA to remain in the B form. After this, free proteins were then rapidly removed from the detection chamber by changing the buffer. Protein dissociation could be monitored by the stepwise decrease in the fluorescence intensity of the acceptor (Figure S12). As summarized in Figure 3a, a dramatic discrimination between B- and Z-DNA was observed in the dissociation step (with dissociation times of only 4.4 s for B-DNA but many hours for Z-DNA), reflecting the “conformational selection” mechanism.

To understand the origin of the Z-DNA specificity of ZBPs more deeply, we performed a study of a mutant hZα_{ADAR1} protein. The previous X-ray crystal structure of a Z-DNA complexed with hZα_{ADAR1} proteins showed that the tyrosine residue at the position 177 forms a CH-π interaction directly with the guanine base in the Z-form of the CG repeats.³¹ To investigate the importance of the hydroxyl group of Tyr-177 in the Z-DNA specificity, we performed buffer exchange experiments with a mutant in which the tyrosine was replaced with a phenylalanine, hZα_{Y177F}, in the same way as in Figure 3a.

Consistent with the expectation, the dissociation time of hZα_{Y177F} from Z-DNA was greatly reduced (Figure 3b and Figure S13), confirming that the interaction between the tyrosine and the guanine base is crucial for the Z-DNA specificity of hZα_{ADAR1}. However, the fact that the Z-DNA stabilizing capability of hZα_{Y177F} was not completely abolished (Figure S14) indicates that other interactions between hZα_{ADAR1} residues and the Z-DNA backbone are still important for the protein's high specificity to Z-DNA.

In summary, we have demonstrated that ZBPs stabilize Z-DNAs via the “conformational selection” mechanism rather than the “induced fit” mechanism. The conformational selection mechanism of ZBPs evidenced in this work may have an implication for the study of other DNA-deformation-inducing proteins:³² the dynamic nature of DNA structure has a critical role in the genome-wide search for the recognition sites by proteins. Such a recognition process is initiated by thermally induced spontaneous fluctuations of DNA structures rather than by active participation of proteins.

■ ASSOCIATED CONTENT

S Supporting Information. Materials, detailed experimental methods, and supplementary figures. This material is available free of charge via the Internet at <http://pubs.acs.org>.

■ AUTHOR INFORMATION

Corresponding Author

kkim@med.skku.ac.kr; ygkimmit@skku.edu; shohng@snu.ac.kr

■ ACKNOWLEDGMENT

This work was supported by the Korea Research Foundation (Grant KRF-2007-331-C00128 to S.H.), the Creative Research Initiatives (Physical Genetics Laboratory, 2009-0081562 to S.H.), the World Class University Project (R31-2009-100320 to S.H.), and the National Research Laboratory Program (NRL-2006-02287 to K.K.K.). S.B. was partly supported by the Seoul R&BD Program.

■ REFERENCES

- (1) Fisher, E. *Dtsch. Chem. Ges.* **1894**, *27*, 2984–2993.
- (2) Klimasauskas, S.; Kumar, S.; Roberts, R. J.; Cheng, X. *Cell* **1994**, *76*, 357–369.
- (3) Kim, Y.; Geiger, J. H.; Hahn, S.; Sigler, P. B. *Nature* **1993**, *365*, 512–520.
- (4) Winkler, F. K.; Banner, D. W.; Oefner, C.; Tsernoglou, D.; Brown, R. S.; Heathman, S. P.; Bryan, R. K.; Martin, P. D.; Petratos, K.; Wilson, K. S. *EMBO J.* **1993**, *12*, 1781–1795.
- (5) Koshland, D. E. *Proc. Natl. Acad. Sci. U.S.A.* **1958**, *44*, 98–104.
- (6) Bosshard, H. R. *News Physiol. Sci.* **2001**, *16*, 171–173.
- (7) Bui, J. M.; McCammon, J. A. *Proc. Natl. Acad. Sci. U.S.A.* **2006**, *103*, 15451–15456.
- (8) Arora, K.; Brooks, C. L., III. *Proc. Natl. Acad. Sci. U.S.A.* **2007**, *104*, 18496–18501.
- (9) Okazaki, K.; Takada, S. *Proc. Natl. Acad. Sci. U.S.A.* **2008**, *105*, 11182–11187.
- (10) Sullivan, S. M.; Holyoak, T. *Proc. Natl. Acad. Sci. U.S.A.* **2008**, *105*, 13829–13834.
- (11) Hammes, G. G.; Chang, Y.-C.; Oas, T. G. *Proc. Natl. Acad. Sci. U.S.A.* **2009**, *106*, 13737–13741.
- (12) Wlodarski, T.; Zagrovic, B. *Proc. Natl. Acad. Sci. U.S.A.* **2009**, *106*, 19346–19351.

- (13) Watson, J. D.; Crick, F. H. C. *Nature* **1953**, *171*, 737–738.
- (14) Wang, A. H.-J.; Quigley, G. J.; Kolpak, F. J.; Crawford, J. L.; van Boom, J. H.; van der Marel, G.; Rich, A. *Nature* **1979**, *282*, 680–686.
- (15) Rich, A.; Zhang, S. *Nat. Rev. Genet.* **2003**, *4*, 566–572.
- (16) Pohl, F. M.; Jovin, J. M. *J. Mol. Biol.* **1972**, *67*, 375–396.
- (17) Singleton, C. K.; Klysik, J.; Stirdivant, S. M.; Wells, R. D. *Nature* **1982**, *299*, 312–316.
- (18) Herbert, A.; Alfken, J.; Kim, Y. G.; Mian, I. S.; Nishikura, K.; Rich, A. *Proc. Natl. Acad. Sci. U.S.A.* **1997**, *94*, 8421–8426.
- (19) Schwartz, T.; Behlke, J.; Lowenhaupt, K.; Heinemann, U.; Rich, A. *Nat. Struct. Biol.* **2001**, *8*, 761–765.
- (20) Rothenburg, S.; Deigendesch, N.; Dittmar, K.; Koch-Nolte, F.; Haag, F.; Lowenhaupt, K.; Rich, A. *Proc. Natl. Acad. Sci. U.S.A.* **2005**, *102*, 1602–1607.
- (21) Ha, S. C.; Kim, D.; Hwang, H.-Y.; Rich, A.; Kim, Y.-G.; Kim, K. K. *Proc. Natl. Acad. Sci. U.S.A.* **2008**, *105*, 20671–20676.
- (22) Kang, Y.-M.; Bang, J.; Lee, E.-H.; Ahn, H.-C.; Seo, Y.-J.; Kim, K. K.; Kim, Y.-G.; Choi, B.-S.; Lee, J.-H. *J. Am. Chem. Soc.* **2009**, *131*, 11485–11491.
- (23) Ha, T.; Enderle, Th.; Ogletree, D. F.; Chemla, D. S.; Selvin, P. R.; Weiss, S. *Proc. Natl. Acad. Sci. U.S.A.* **1996**, *93*, 6264–6268.
- (24) Roy, R.; Hohng, S.; Ha, T. *Nat. Methods* **2008**, *5*, 507–516.
- (25) Lee, M.; Kim, S. H.; Hong, S.-C. *Proc. Natl. Acad. Sci. U.S.A.* **2010**, *107*, 4985–4990.
- (26) Ha, S. C.; Lowenhaupt, K.; Rich, A.; Kim, Y.-G.; Kim, K. K. *Nature* **2005**, *437*, 1183–1186.
- (27) Myong, S.; Cui, S.; Cornish, P. V.; Kirchhofer, A.; Gack, M. U.; Jung, J. U.; Hopfner, K.-P.; Ha, T. *Science* **2009**, *323*, 1070–1074.
- (28) Behe, M.; Zimmerman, S.; Felsenfeld, G. *Nature* **1981**, *293*, 233–235.
- (29) Adam, S.; Bourtayre, P.; Liquier, J.; Taillandier, E. *Nucleic Acids Res.* **1986**, *14*, 3501–3513.
- (30) Ha, S. C.; Lokanath, N. K.; Van Quyen, D.; Wu, C. A.; Lowenhaupt, K.; Rich, A.; Kim, Y. G.; Kim, K. K. *Proc. Natl. Acad. Sci. U.S.A.* **2004**, *101*, 14367–14372.
- (31) Schwartz, T.; Rould, M. A.; Lowenhaupt, K.; Herbert, A.; Rich, A. *Science* **1999**, *284*, 1841–1845.
- (32) Parker, J. B.; Bianchet, M. A.; Krosky, D. J.; Friedman, J. I.; Amzel, L. M.; Stivers, J. T. *Nature* **2007**, *449*, 433–437.